Supplementary Figure S1

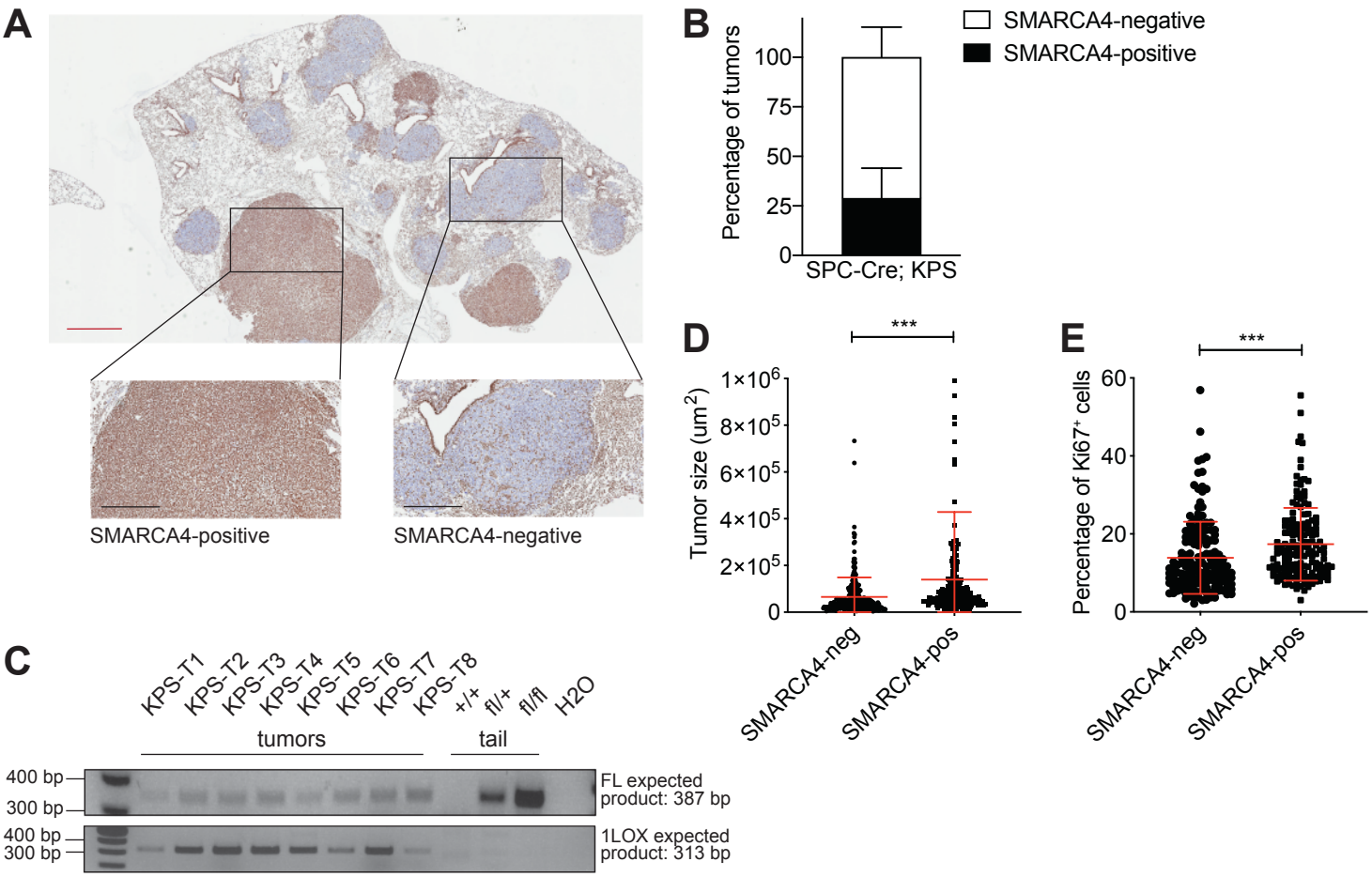

Supplementary Figure S1. A fraction of tumors initiated from SPC⁺ cells in KPS animals retain SMARCA4 expression.

(A) Representative SMARCA4 staining of a tumor-bearing lung from a KPS animal infected with Ad-SPC-Cre showing retained SMARCA4 expression in multiple tumors. Red scale bar: 1 mm; black scale bars: 500 μm. **(B)** Quantification of the percentage of SMARCA4-postive and –negative tumors in the lungs of KPS animals (n=8) infected with Ad-SPC-Cre. Data are mean ± s.d. **(C)** Genotyping PCR of laser-capture microdissected SMARCA4-positive tumors from KPS animals detecting the *Smarca4* floxed (387 bp) and recombined (313 bp) alleles. **(D)** Quantification of SMARCA4-negative and –positive tumor size in KPS animals. Red lines are mean ± s.d. Student's two-tailed unpaired t-test: ***p = 0.0001. **(E)** Quantification of the percentage of Ki67-positive cells in SMARCA4-negative and –positive tumors in KPS animals. Red lines are mean ± s.d. Student's two-tailed unpaired t-test: ***p = 0.0009.

Supplementary Figure S2

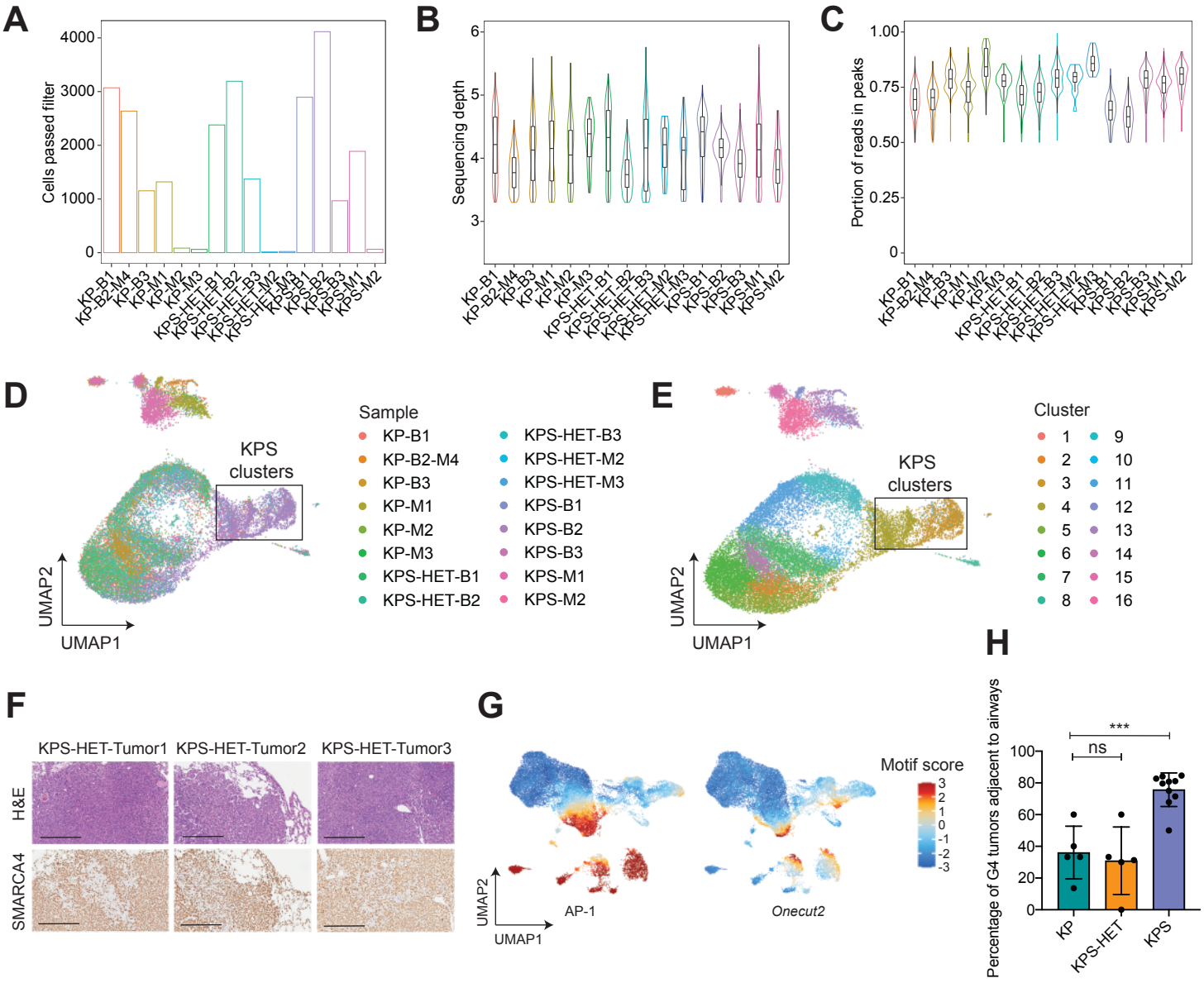

Supplementary Figure S2. The chromatin accessibility profiles and features of *Smarca4*-deficient murine lung adenocarcinomas initiated from SPC-expressing cells.
Quality control metrics for scATAC-seq dataset showing: **(A)** number of cells per sample passing quality control filters; **(B)** sequencing depth per sample; **(C)** fraction of reads in peaks. UMAP projection of chromatin accessibility profiles reduced using chromVAR colored by **(D)** sample and **(E)** cluster. Clusters specific to KPS samples are boxed. **(F)** H&E and SMARCA4 staining of KPS-HET tumors with SMARCA4-negative cancer cells. Scale bar: 300 µm. **(G)** UMAP projection of scATAC-seq dataset colored by AP-1 and *Onecut2* motif scores. **(H)** Percentage of Grade 4 tumors located adjacent to airways in KP (n=5), KPS-HET (n=5), and KPS (n=10) animals. Data are mean ± s.d. One-way ANOVA: $F(2, 17) = 19.45$, $p < 0.0001$; Dunnett's multiple comparisons test: ****adjusted p-value* = 0.0004.

Supplementary Figure S3

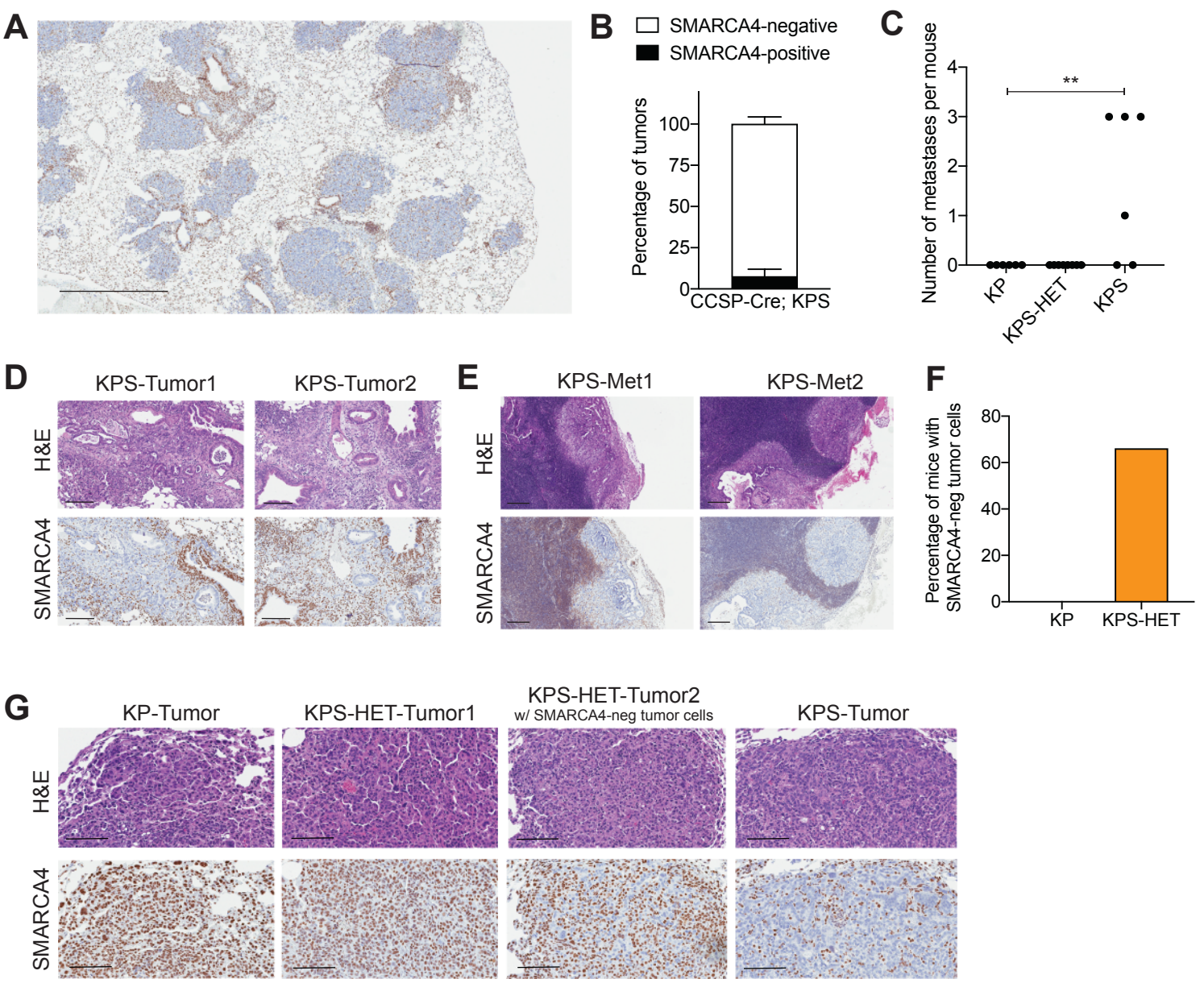

Supplementary Figure S3. Loss of SMARCA4 expression in tumors initiated from CCSP^{+} cells in KPS animals.
(A) Representative SMARCA4 staining of a tumor-bearing lung from a KPS animal infected with Ad-CCSP-Cre. Scale bar: 1 mm. **(B)** Quantification of percentage of SMARCA4-positive and –negative tumors in the lungs of KPS animals (n=5) infected with Ad-CCSP-Cre. Data are mean ± s.d. **(C)** Quantification of the number of micro-metastases observed per mouse in KP (n=6), KPS-HET (n=8), and KPS (n=6) animals 16 weeks post-infection. One-way ANOVA: $F(2, 17) = 8.750$, $p = 0.0024$; Dunnett's multiple comparisons test: ***adjusted p-value* = 0.0048. **(D)** Representative H&E and SMARCA4 staining of Grade 4 tumors in KPS animals. Scale bars: 150 μm. **(E)** Representative H&E and SMARCA4 staining of metastases in KPS animals. Scale bars: 250 μm. **(F)** Percentage of KPS-HET animals (n=8) having SMARCA4-negative tumor cells 16 weeks post-infection. **(G)** Representative H&E and SMARCA4 staining of tumors in KP, KPS-HET, and KPS animals showing the presence of SMARCA4-negative cancer cells in KPS-HET tumors. Scale bars: 100 um.

Supplementary Figure S4

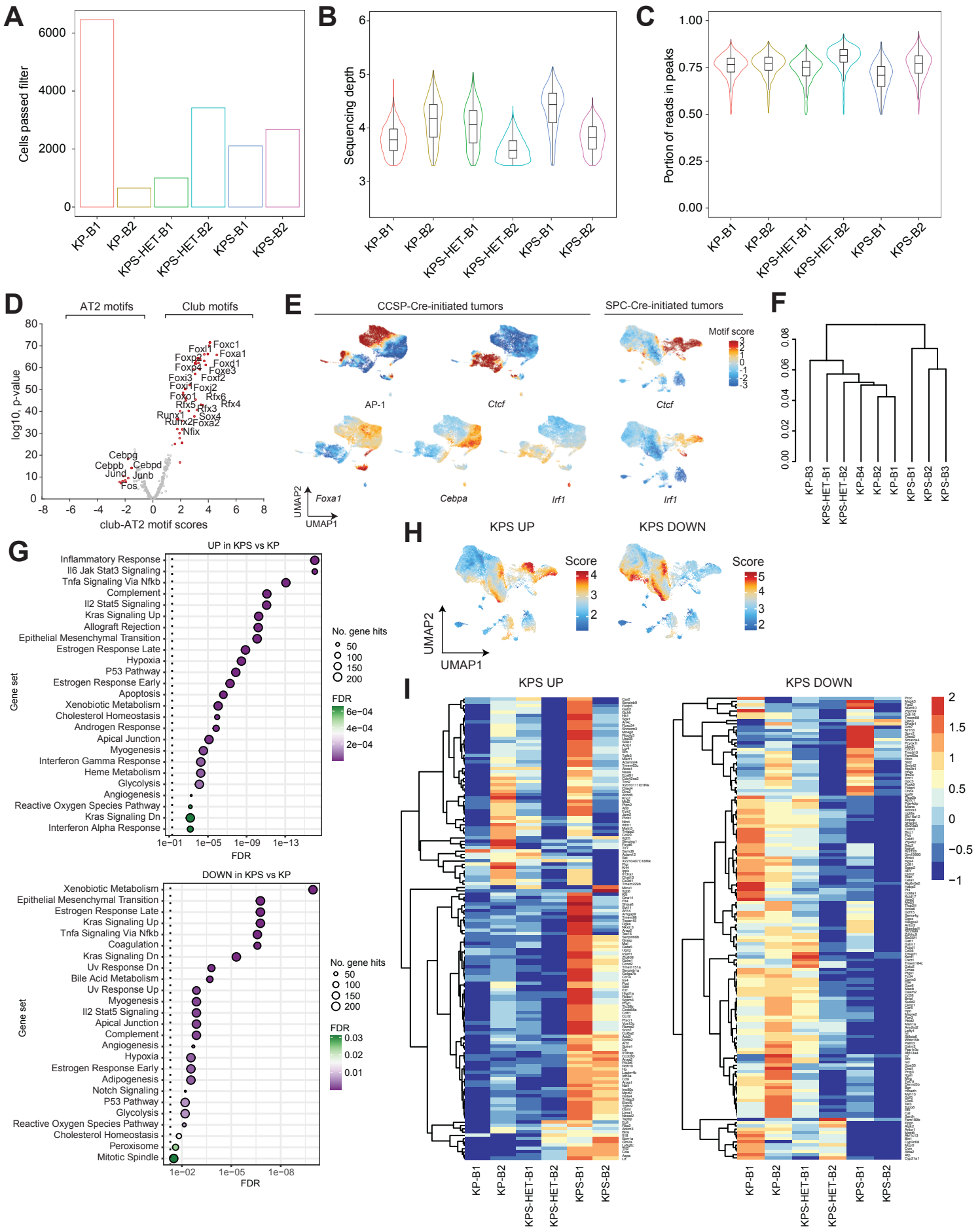

Supplementary Figure S4. The chromatin accessibility profiles and features of *Smarca4*-deficient murine lung adenocarcinomas initiated from CCSP-expressing cells.
Quality control metrics for scATAC-seq dataset showing: **(A)** number of cells per sample passing quality control filters; **(B)** sequencing depth per sample and; **(C)** fraction of reads in peaks. **(D)** Differentially accessible motifs between normal club and AT2 cells. **(E)** UMAP projection of murine scATAC-seq datasets colored by normalized motif scores of selected TFs. **(F)** Unsupervised hierarchical clustering of RNA-seq samples from KP (n=4), KPS-HET (n=2), and KPS (n=3) primary tumors. **(G)** Dot plot of enriched hallmark gene sets in genes with increased (upper panel) and decreased (lower panel) expression (*adjusted p-value* < 0.05, |FC|>1.5) in KPS primary tumors (n=3) compared to KP (n=4) primary tumors. Dots are sized on the log10 scale of the number of genes in each hallmark gene set. Size legend shows raw number of genes. **(H)** UMAP visualization of the SPC scATAC-seq dataset colored by mean gene score of differential genes increased and decreased (*adjusted p-value* < 0.05, |FC|>1.5) in KPS primary tumors (n=3) compared to KP (n=4) primary tumors. **(I)** Heatmaps showing the mean gene scores of differential genes identified through RNA-seq in each CCSP scATAC-seq sample ($p < 0.00001$).

Supplementary Figure S5

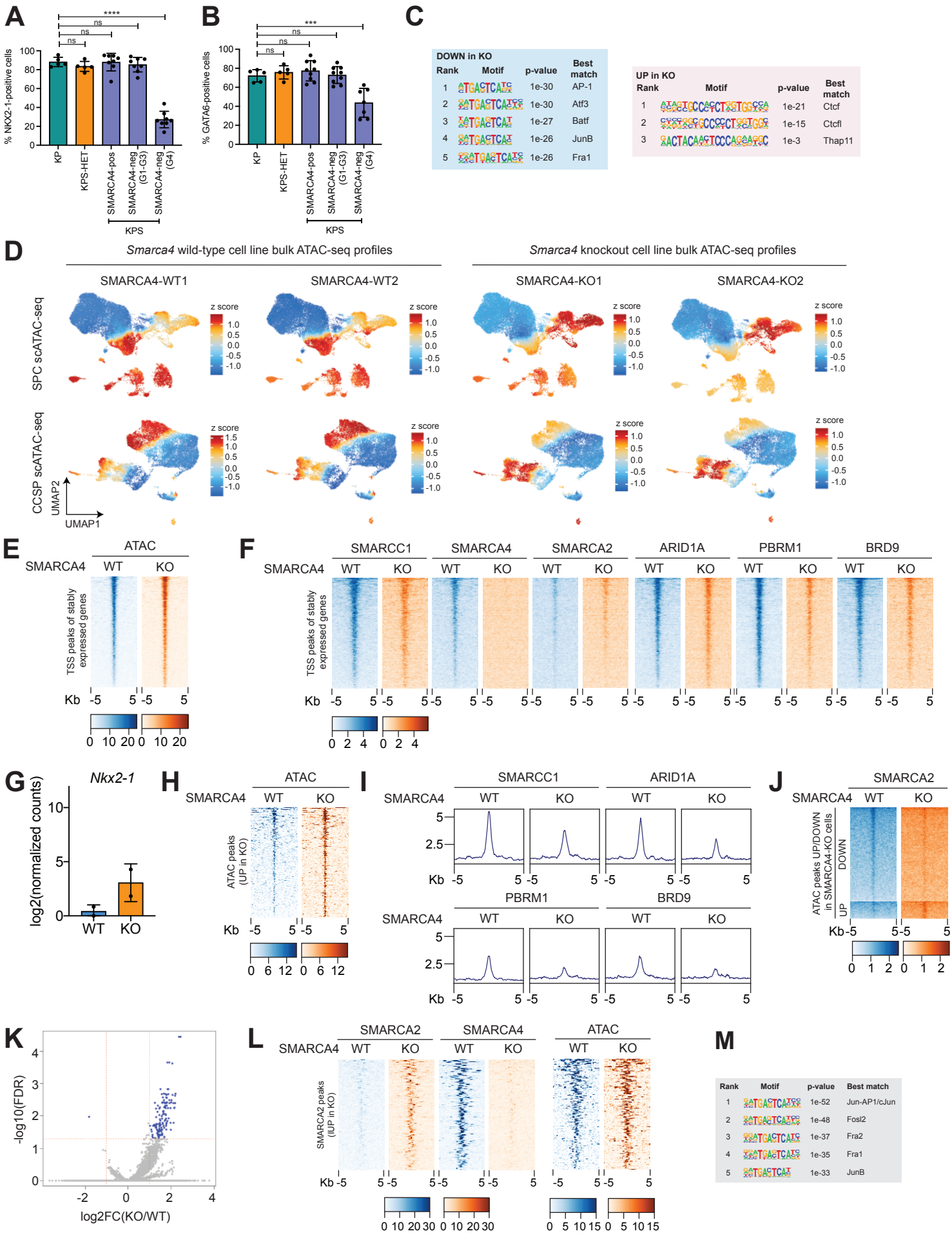

Supplementary Figure S5. SWI/SNF function upon *Smarca4* inactivation.
(A) Quantification of NKX2-1 staining in lung tumors initiated from SPC^+ cells in KP (n=5), KPS-HET (n=5), and KPS (n=8) animals (grouped by SMARCA4 protein expression status and histological tumor grade). The average percentage of NKX2-1-positive cells per tumor in each mouse is shown. Data are mean ± s.d. One-way ANOVA: $F(4, 29) = 88.68$, $p < 0.0001$; Dunnett's multiple comparisons test: ****$adjusted\ p\text{-}value < 0.0001$. **(B)** Quantification of GATA6 staining in lung tumors initiated from SPC^+ cells in KP (n=5), KPS-HET (n=5), and KPS animals (grouped by SMARCA4 protein expression status and histological tumor grade where n=9 for SMARCA4-positive and SMARCA4-negative G1-G3 tumors and n=7 for SMARCA4-negative Grade 4 tumors). The average percentage of GATA6-positive cells per tumor in each mouse is shown. Data are mean ± s.d. One-way ANOVA: $F(4, 30) = 12.65$, $p < 0.0001$; Dunnett's multiple comparisons test: ***$adjusted\ p\text{-}value = 0.0002$. **(C)** Top motifs enriched in differential ATAC-seq peaks at distal intergenic regions between SMARCA4-WT and –KO cells. **(D)** UMAP visualization of the scATAC-seq datasets colored by z score for bulk ATAC-seq peak sets of SMARCA4-WT and –KO isogenic cells. **(E)** Representative ATAC-seq density heatmaps showing chromatin accessibility at TSS peaks of stably expressed genes between SMARCA4-WT and –KO cell lines. **(F)** Representative CUT&RUN density heatmaps showing occupancies of SWI/SNF subunits at TSS peaks of stably expressed genes between SMARCA4-WT and –KO cell lines. **(G)** Transcript levels of *Nkx2-1* in SMARCA4-WT and –KO cell lines in RNA-seq dataset. *Nkx2-1* is not differentially expressed ($p_{DE} = 0.1398$ by DESeq2). **(H)** Representative ATAC-seq density heatmaps showing chromatin accessibility of differential ATAC-seq peaks at distal intergenic regions significantly increased in SMARCA4-KO LUAD. **(I)** Representative CUT&RUN density metaplots showing occupancies of the pan-SWI/SNF component SMARCC1 and SWI/SNF class-specific components ARID1A (cBAF), PBRM1 (PBAF), and BRD9 (ncBAF/GBAF) at differential ATAC-seq peaks at distal intergenic regions significantly increased in SMARCA4-KO LUAD. **(J)** Representative SMARCA2 CUT&RUN density heatmaps showing SMARCA2 occupancy at differential ATAC-seq peaks at distal intergenic regions between SMARCA4-WT and –KO LUAD. **(K)** Volcano plot showing differential SMARCA2 CUT&RUN peaks in SMARCA4-WT and –KO cells. Red lines indicate FDR < 0.05 and |log2FC| >1 thresholds. **(L)** Representative SMARCA2 and SMARCA4 CUT&RUN and ATAC-seq density heatmaps showing SMARCA2 and SMARCA4 occupancies and chromatin accessibility at differential SMARCA2 peaks significantly increased in SMARCA4-KO LUAD (FDR < 0.05). **(M)** Top motifs detected in significantly enriched SMARCA2 peaks (FDR < 0.05) in SMARCA4-KO cells.

Supplementary Figure S6

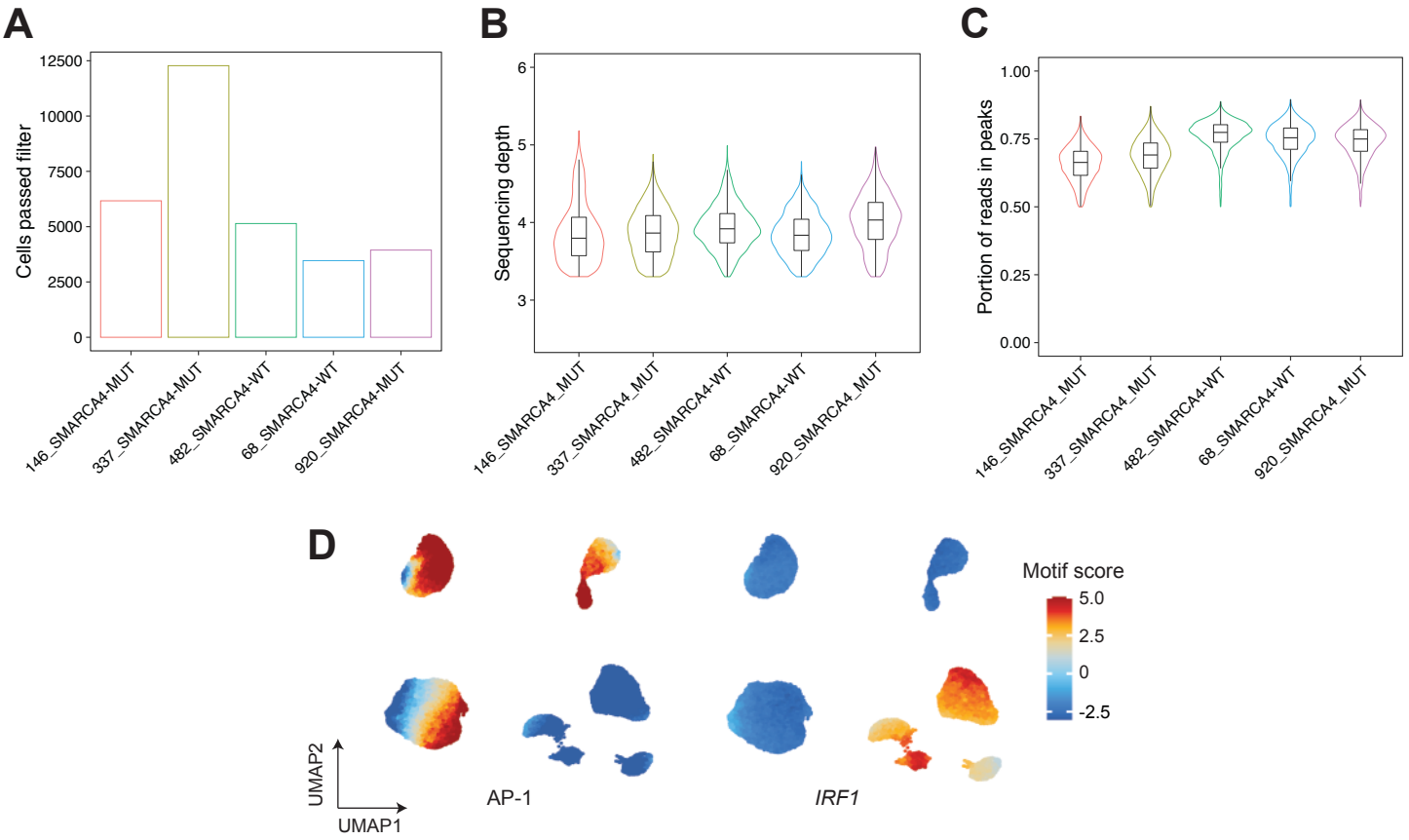

Supplementary Figure S6. The chromatin accessibility profiles and features of *Smarca4*-mutant human LUAD. Quality control metrics for scATAC-seq dataset showing: **(A)** number of cells per sample passing quality control filters; **(B)** sequencing depth per sample and; **(C)** fraction of reads in peaks. **(D)** UMAP projection of LUAD PDX scATAC-seq dataset colored by normalized motif scores of AP-1 and *IRF1*.

Supplementary Figure S7

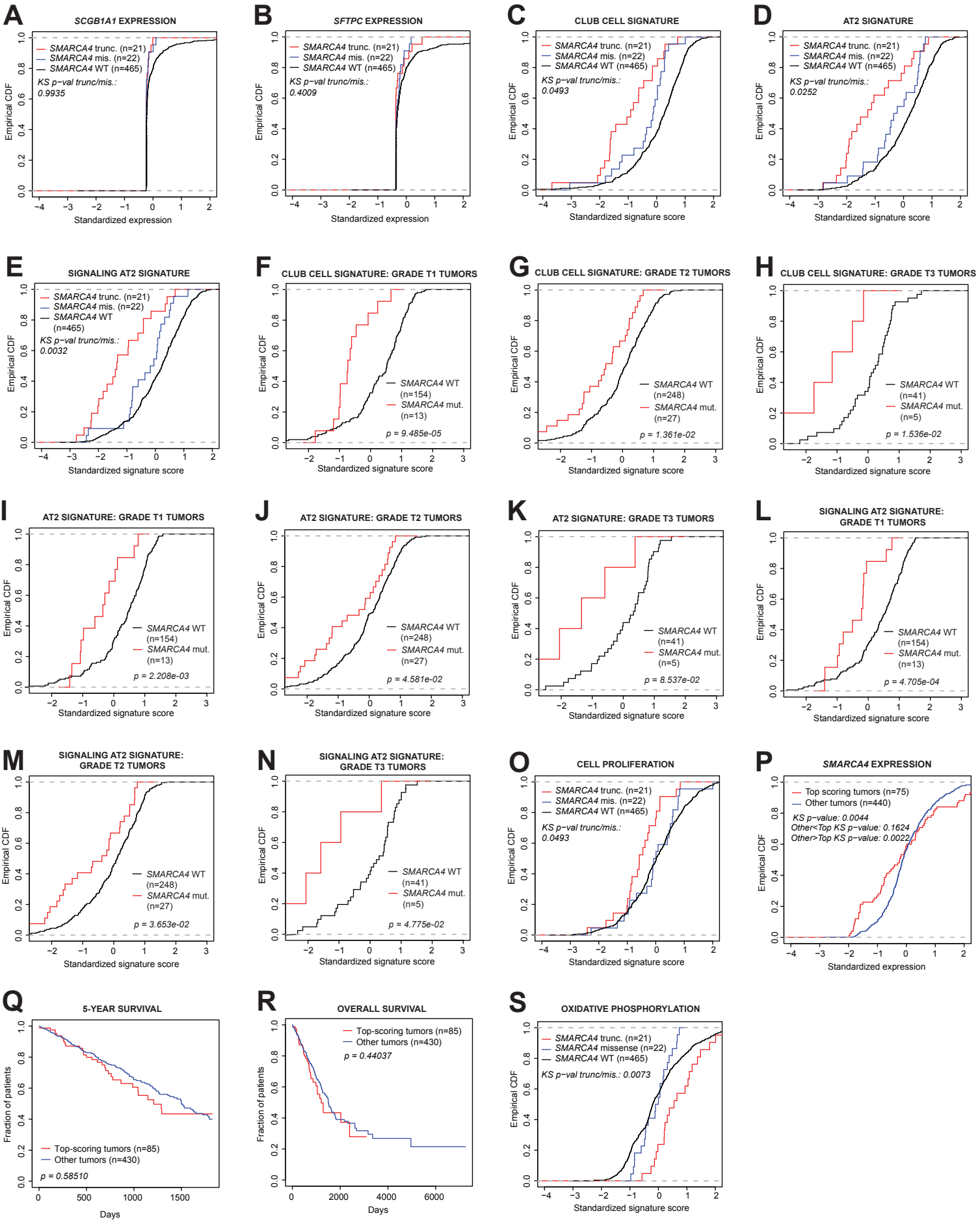

Supplementary Figure S7. Lineage, ESC-like, and KPS signatures in *SMARCA4*-mutant TCGA LUAD patients. Empirical CDF plots of standardized *SCGB1A1* **(A)** and *SFTPC* **(B)** expression in *SMARCA4*-wild-type (WT), missense, and truncating mutant TCGA LUAD. Empirical CDF plots of standardized SS2 club cell **(C)**, AT2 **(D)**, and signaling AT2 **(E)** signature scores in TCGA LUAD with intact *SMARCA4* (WT), *SMARCA4* missense mutations, and *SMARCA4* truncating mutations. Empirical CDF plots of standardized 10x club cell **(F-H)**, AT2 **(I-K)**, and signaling AT2 **(L-N)** signature scores in TCGA LUAD with intact (WT) and mutant (mut) *SMARCA4* grouped by tumor grade. **(O)** Empirical CDF plots of standardized proliferation signature (GO_8283) scores in TCGA LUAD with intact *SMARCA4* (WT), *SMARCA4* missense mutations, and *SMARCA4* truncating mutations. **(P)** Empirical CDF plot comparing standardized *SMARCA4* expression between top-scoring TCGA LUAD correlated to the ESC-like signature ($z > 1$) and the rest of the cohort. **(Q)** 5-year and **(R)** overall Kaplan-Meier survival curves of the top TCGA LUAD patients correlated with KPS signature ($z > 1$) compared with the rest of the cohort. **(S)** Empirical CDF plots of standardized oxidative phosphorylation signature scores in TCGA LUAD with intact *SMARCA4* (WT), *SMARCA4* missense mutations, and *SMARCA4* truncating mutations.